

# Galvano- and thermo-magnetic effects at low and high temperatures within non-Markovian quantum Langevin approach

I.B. Abdurakhmanov<sup>1</sup>, G.G. Adamian<sup>2</sup>, N.V. Antonenko<sup>2</sup>, and Z. Kanokov<sup>2,3,4</sup>

<sup>1</sup>*Curtin Institute for Computation, Department of Physics,  
Astronomy and Medical Radiation Sciences,  
Curtin University, Perth, WA 6845, Australia*

<sup>2</sup>*Joint Institute for Nuclear Research, 141980 Dubna, Russia*

<sup>3</sup>*National University, 700174 Tashkent, Uzbekistan*

<sup>4</sup>*Institute of Nuclear Physics, 702132 Tashkent, Uzbekistan*

(Dated: June 6, 2018)

## Abstract

The quantum Langevin formalism is used to study the charge carrier transport in a two-dimensional sample. The center of mass of charge carriers is visualized as a quantum particle, while an environment acts as a heat bath coupled to it through the particle-phonon interaction. The dynamics of the charge carriers is limited by the average collision time which takes effectively into account the two-body effects. The functional dependencies of particle-phonon interaction and average collision time on the temperature and magnetic field are phenomenologically treated. The galvano-magnetic and thermo-magnetic effects in the quantum system appear as the result of the transitional processes at low temperatures.

PACS numbers: 09.37.-d, 03.40.-a, 03.65.-w, 24.60.-k

Keywords: Classical and Quantum Hall effect; Shubnikov-De Haas effect; cyclotron frequency; friction coefficients; Langevin formalism; non-Markovian dynamics; electric and magnetic field

## I. INTRODUCTION

The behavior of solid matter under the influence of external fields at low temperature is one of the interesting topics in solid-state physics [1–3]. The external field may be an electric field, magnetic field, optical signal, or temperature gradient. These fields modify some electronic properties, such as the carrier concentration and the carrier mobility. Besides the carrier mobility, the electric current is also affected by the magnetic field which deflects its direction and leads to a nonzero cross voltage (the classical Hall effect) linearly proportional to the field strength [1–4]. The oscillator nature of the longitudinal magneto-resistance of bismuth sample at low temperature, known as the Shubnikov-De Haas effect, has been also observed in the presence of very intense magnetic fields [1, 3, 5, 6]. The effect is more pronounced at low temperatures where the amplitude of oscillations is significantly larger. The first experimental study of the influence of electric fields of the order of  $100 \text{ mV cm}^{-1}$  on the Shubnikov-de Haas magneto-resistance oscillations in  $n$ -InSb sample has been reported in Ref. [5]. In addition to the shift of the extremes to higher magnetic fields, a decrease of oscillation amplitudes with electric field has been observed. The Integer Quantum Hall Effect (IQHE) in the GaAs-Al<sub>0.3</sub>Ga<sub>0.7</sub>As heterostructure has been discovered [7, 8] at strong external electromagnetic fields and very low temperature. The quantization of conductivity surprisingly occurred in a certain two-dimensional electron gas (2DEG) under the influence of a strong magnetic field. In the IQHE, the Hall conductance  $\sigma_{xy}$  has a stepwise dependence (the appearance of plateau) on the strong external magnetic field. At these plateau,  $\sigma_{xy}$  is quantized as  $\sigma_{xy} = ie^2/(2\pi\hbar)$ ,  $i = 1, 2, \dots$ , while the longitudinal conductivity  $\sigma_{xx}$  nearly vanishes. The vanishing  $\sigma_{xx}$  implies the absence of dissipation. This is another hallmark of the IQHE. Also, the Fractional Quantum Hall Effect (FQHE), where the Hall conductivity is quantized in fractional multiples of  $e^2/(2\pi\hbar)$ , has been discovered [9, 10].

The theoretical models in Refs. [11–15] for describing the IQHE and FQHE have been developed. The combination of a random potential created by impurities in a sample and strong magnetic field gives rise to the special coexistence of localized and extended electron states. As known, the Fermi level lies in the energy gap (mobility gap) free from the extended states and the change of the electron density or the magnetic field can only result in different occupations of localized states which do not affect the conductivity. Based on these findings the appearance of the conductivity quantization has been explained. The general approach,

which explains the quantization as well as the integer quantized values, has been developed later with the scaling theory. This approach also describes correctly the regions where the conductivity is not quantized [11]. For the theoretical explanation of the FQHE, the wave functions have been introduced [12] to describe the incompressible quantum states and explain the small but experimentally prominent class of fractions  $1/\text{odd}$ . It turned out that the quasiparticle excitations are the charge/fluxcomposites with a fractional charge and statistics, also known as dubbed anyons. The special properties of charge/fluxcomposites have been used in Refs. [13–15] to construct two so-called hierarchies, sets of Hall fractions for which the incompressible ground states could be found. These hierarchies are able to reproduce all fractions observed, but also yield many fractions that have never been measured. The striking universality in the manifestation of the quantum Hall effect attracted large attention, not only in solid state physics but also in high energy physics. The extensive mathematical methods of topological field theory [16] and infinite dimensional algebras [17–19] have been applied to the IQHE and FQHE. As found in several independent works, the description of incompressible quantum states exploits the theory of chiral edge currents [17]. The Quantum Hall ground states and quasiparticle excitations have been described in terms of representations of the infinite-dimensional algebras [17–19].

The aim of the present work is to treat the classic and quantum Hall effect as well as the Shubnikov-De Haas effect within the same model. The basic idea of our model is the following. In the electric current, we determine the time-dependent number of electrons with given momentum at a certain location. We consider the center of mass of charge carriers with a positive charge  $e = |e|$  as a quantum particle coupled to the environment (heat bath) through the particle-phonon interactions. Solving the second order Heisenberg equations for the heat bath degrees of freedom, the generalized non-Markovian Langevin equations are explicitly obtained for a quantum particle. The memory effects in these equations results from the coupling to the environment. The dynamics of the charge carriers is restricted by the average collision time. The functional form of the particle-phonon coupling strength and the average collision time on the temperature and magnetic field are phenomenologically treated.

The paper is organized as follows. In Sec. II, we introduce the Hamiltonian of the system and solve the generalized non-Markovian Langevin equations for a quantum particle. The electric and thermal conductivities are derived in two-dimensional systems. Note that the

quantum Langevin approach or the density matrix formalism has been widely applied to find the effects of fluctuations and dissipation in macroscopic systems [20–47]. The main assumptions of the model are discussed. The model developed is used in Sec. III to describe the experimental data on the classic and quantum Hall and Shubnikov-De Haas effects. A summary is given in Sec. IV.

## II. NON-MARKOVIAN LANGEVIN EQUATIONS WITH EXTERNAL MAGNETIC AND ELECTRIC FIELDS

### A. Derivation of quantum Langevin equations

Let us consider two-dimensional motion of a quantum charge particle in the presence of heat bath and external constant electric  $\mathbf{E} = (E_x, 0, 0)$  and magnetic fields  $\mathbf{B} = (0, 0, B)$ . The total Hamiltonian of this system is

$$H = H_c + H_b + H_{cb}. \quad (1)$$

The Hamiltonian  $H_c$  describes the collective subsystem (quantum particle) with effective mass tensor and charge  $e = |e|$  in electric and magnetic fields:

$$H_c = \frac{1}{2m_x} [p_x - eA_x(x, y)]^2 + \frac{1}{2m_y} [p_y - eA_y(x, y)]^2 + eE_x x = \frac{\pi_x^2}{2m_x} + \frac{\pi_y^2}{2m_y} + eE_x x. \quad (2)$$

Here,  $m_x$  and  $m_y$  are the components of the effective mass tensor,  $\mathbf{R} = (x, y, 0)$  and  $\mathbf{p} = (p_x, p_y, 0)$  are the coordinate and canonically conjugated momentum, respectively,  $\mathbf{A} = (-\frac{1}{2}yB, \frac{1}{2}xB, 0)$  is the vector potential of the magnetic field, and the electric field  $E_x$  acts in  $x$  direction. For simplicity, in Eq. (2) we introduce the notations

$$\pi_x = p_x + \frac{1}{2}m_x\omega_{cx}y, \quad \pi_y = p_y - \frac{1}{2}m_y\omega_{cy}x$$

with frequencies  $\omega_{cx} = \frac{eB}{m_x}$  and  $\omega_{cy} = \frac{eB}{m_y}$ . The cyclotron frequency is  $\omega_c = \sqrt{\omega_{cx}\omega_{cy}} = \frac{eB}{\sqrt{m_x m_y}}$ .

The second term in Eq. (1) represents the Hamiltonian of the phonon heat bath

$$H_b = \sum_{\nu} \hbar\omega_{\nu} b_{\nu}^{\dagger} b_{\nu}, \quad (3)$$

where  $b_{\nu}^{\dagger}$  and  $b_{\nu}$  are the phonon creation and annihilation operators of the heat bath. The coupling between the heat bath and collective subsystem is described by

$$H_{cb} = \sum_{\nu} V_{\nu}(\mathbf{R})(b_{\nu}^{\dagger} + b_{\nu}) + \sum_{\nu} \frac{1}{\hbar\omega_{\nu}} V_{\nu}^2(\mathbf{R}). \quad (4)$$

The first term in Eq. (4) corresponds to the energy exchange between the collective subsystem and heat bath. We introduce the counterterm (second term) in  $H_{cb}$  to compensate the coupling-induced renormalization of the collective potential. Naturally, it can be always separated from  $eE_x x$  in Eq. (2). In general case,  $V_\nu(\mathbf{R})$  depends on the strength of magnetic field and an impact of  $\mathbf{B}$  is entered into the dissipative kernels and random forces.

The equations of two-dimensional motion are

$$\begin{aligned}\dot{x}(t) &= \frac{i}{\hbar}[H, x] = \frac{\pi_x(t)}{m_x}, & \dot{y}(t) &= \frac{i}{\hbar}[H, y] = \frac{\pi_y(t)}{m_y}, \\ \dot{\pi}_x(t) &= \frac{i}{\hbar}[H, \pi_x] = \pi_y(t)\omega_{cy} - eE_x - \sum_\nu V'_{\nu,x}(\mathbf{R})(b_\nu^+ + b_\nu) - 2 \sum_\nu \frac{V_\nu(\mathbf{R})V'_{\nu,x}(\mathbf{R})}{\hbar\omega_\nu}, \\ \dot{\pi}_y(t) &= \frac{i}{\hbar}[H, \pi_y] = -\pi_x(t)\omega_{cx} - \sum_\nu V'_{\nu,y}(\mathbf{R})(b_\nu^+ + b_\nu) - 2 \sum_\nu \frac{V_\nu(\mathbf{R})V'_{\nu,y}(\mathbf{R})}{\hbar\omega_\nu},\end{aligned}\quad (5)$$

and

$$\begin{aligned}\dot{b}_\nu^+(t) &= \frac{i}{\hbar}[H, b_\nu^+] = i\omega_\nu b_\nu^+(t) + \frac{i}{\hbar}V_\nu(\mathbf{R}), \\ \dot{b}_\nu(t) &= \frac{i}{\hbar}[H, b_\nu] = -i\omega_\nu b_\nu(t) - \frac{i}{\hbar}V_\nu(\mathbf{R}).\end{aligned}\quad (6)$$

The solution of Eqs. (6) are

$$\begin{aligned}b_\nu^+(t) + b_\nu(t) &= f_\nu^+(t) + f_\nu(t) - \frac{2V_\nu(\mathbf{R})}{\hbar\omega_\nu} + \frac{2}{\hbar\omega_\nu} \int_0^t d\tau \dot{V}_\nu(\mathbf{R}(\tau)) \cos(\omega_\nu[t - \tau]), \\ b_\nu^+(t) - b_\nu(t) &= f_\nu^+(t) - f_\nu(t) + \frac{2i}{\hbar\omega_\nu} \int_0^t d\tau \dot{V}_\nu(\mathbf{R}(\tau)) \sin(\omega_\nu[t - \tau]),\end{aligned}\quad (7)$$

where

$$f_\nu(t) = [b_\nu(0) + \frac{1}{\hbar\omega_\nu}V_\nu(\mathbf{R}(0))]e^{-i\omega_\nu t}.$$

Substituting (7) into (5) and eliminating the bath variables from the equations of motion for the collective subsystem, we obtain the set of nonlinear integro-differential stochastic dissipative equations

$$\begin{aligned}\dot{x}(t) &= \frac{\pi_x(t)}{m_x}, & \dot{y}(t) &= \frac{\pi_y(t)}{m_y}, \\ \dot{\pi}_x(t) &= \pi_y(t)\omega_{cy} - eE_x - \frac{1}{2} \int_0^t d\tau \{K_{xx}(t, \tau), \dot{x}(\tau)\}_+ - \frac{1}{2} \int_0^t d\tau \{K_{xy}(t, \tau), \dot{x}(\tau)\}_+ + F_x(t), \\ \dot{\pi}_y(t) &= -\pi_x(t)\omega_{cx} - \frac{1}{2} \int_0^t d\tau \{K_{yy}(t, \tau), \dot{y}(\tau)\}_+ - \frac{1}{2} \int_0^t d\tau \{K_{yx}(t, \tau), \dot{y}(\tau)\}_+ + F_y(t).\end{aligned}\quad (8)$$

The dissipative kernels and random forces in (8) are

$$\begin{aligned}
K_{xx}(t, \tau) &= \sum_{\nu} \frac{1}{\hbar\omega_{\nu}} \{V'_{\nu,x}(\mathbf{R}(t)), V'_{\nu,x}(\mathbf{R}(\tau))\}_+ \cos(\omega_{\nu}[t - \tau]), \\
K_{xy}(t, \tau) &= \sum_{\nu} \frac{1}{\hbar\omega_{\nu}} \{V'_{\nu,x}(\mathbf{R}(t)), V'_{\nu,y}(\mathbf{R}(\tau))\}_+ \cos(\omega_{\nu}[t - \tau]), \\
K_{yx}(t, \tau) &= \sum_{\nu} \frac{1}{\hbar\omega_{\nu}} \{V'_{\nu,y}(\mathbf{R}(t)), V'_{\nu,x}(\mathbf{R}(\tau))\}_+ \cos(\omega_{\nu}[t - \tau]), \\
K_{yy}(t, \tau) &= \sum_{\nu} \frac{1}{\hbar\omega_{\nu}} \{V'_{\nu,y}(\mathbf{R}(t)), V'_{\nu,y}(\mathbf{R}(\tau))\}_+ \cos(\omega_{\nu}[t - \tau])
\end{aligned} \tag{9}$$

and

$$\begin{aligned}
F_x(t) &= \sum_{\nu} F_x^{\nu}(t) = - \sum_{\nu} V'_{\nu,x}(\mathbf{R}(t)) [f_{\nu}^{+}(t) + f_{\nu}(t)], \\
F_y(t) &= \sum_{\nu} F_y^{\nu}(t) = - \sum_{\nu} V'_{\nu,y}(\mathbf{R}(t)) [f_{\nu}^{+}(t) + f_{\nu}(t)],
\end{aligned} \tag{10}$$

respectively. Here, we use the notations:  $V'_{\nu,x} = \partial V_{\nu}/\partial x$ ,  $V'_{\nu,y} = \partial V_{\nu}/\partial y$ , and  $\{Z_1, Z_2\}_+ = Z_1 Z_2 + Z_2 Z_1$ . Following the usual procedure of statistical mechanics, we identify the operators  $F_x^{\nu}$  and  $F_y^{\nu}$  as fluctuations because of the uncertainty of the initial conditions for the bath operators. To specify the statistical properties of fluctuations, we consider an ensemble of initial states in which the fluctuations have the Gaussian distribution with zero average value

$$\ll F_x^{\nu}(t) \gg = \ll F_y^{\nu}(t) \gg = 0. \tag{11}$$

The symbol  $\ll \dots \gg$  denotes the average over the bath with the Bose-Einstein statistics

$$\begin{aligned}
\ll f_{\nu}^{+}(t) f_{\nu'}^{+}(t') \gg &= \ll f_{\nu}(t) f_{\nu'}(t') \gg = 0, \\
\ll f_{\nu}^{+}(t) f_{\nu'}(t') \gg &= \delta_{\nu,\nu'} n_{\nu} e^{i\omega_{\nu}[t-t']}, \\
\ll f_{\nu}(t) f_{\nu'}^{+}(t') \gg &= \delta_{\nu,\nu'} (n_{\nu} + 1) e^{-i\omega_{\nu}[t-t']},
\end{aligned} \tag{12}$$

where the occupation numbers  $n_{\nu} = [\exp(\hbar\omega_{\nu}/T) - 1]^{-1}$  for phonons depend on temperature  $T$  given in energy units.

Using the properties (11) and (12) of random forces, we obtain the following symmetrized

correlation functions  $\varphi_{kk'}^\nu(t, t') = \ll F_k^\nu(t)F_{k'}^\nu(t') + F_{k'}^\nu(t')F_k^\nu(t) \gg (k, k' = x, y)$ :

$$\begin{aligned}
\varphi_{xx}^\nu(t, t') &= [2n_\nu + 1]\{V'_{\nu,x}(\mathbf{R}(t)), V'_{\nu,x}(\mathbf{R}(t'))\}_+ \cos(\omega_\nu[t - t']), \\
\varphi_{yy}^\nu(t, t') &= \varphi_{xx}^\nu(t, t')|_{x \rightarrow y}, \\
\varphi_{xy}^\nu(t, t') &= [2n_\nu + 1]\{V'_{\nu,x}(\mathbf{R}(t)), V'_{\nu,y}(\mathbf{R}(t'))\}_+ \cos(\omega_\nu[t - t']), \\
\varphi_{yx}^\nu(t, t') &= \varphi_{xy}^\nu(t, t')|_{x \rightarrow y}.
\end{aligned} \tag{13}$$

The quantum fluctuation-dissipation relations read

$$\begin{aligned}
\sum_\nu \varphi_{xx}^\nu(t, t') \frac{\tanh[\frac{\hbar\omega_\nu}{2T}]}{\hbar\omega_\nu} &= K_{xx}(t, t'), \\
\sum_\nu \varphi_{yy}^\nu(t, t') \frac{\tanh[\frac{\hbar\omega_\nu}{2T}]}{\hbar\omega_\nu} &= K_{yy}(t, t'), \\
\sum_\nu \varphi_{xy}^\nu(t, t') \frac{\tanh[\frac{\hbar\omega_\nu}{2T}]}{\hbar\omega_\nu} &= K_{xy}(t, t'), \\
\sum_\nu \varphi_{yx}^\nu(t, t') \frac{\tanh[\frac{\hbar\omega_\nu}{2T}]}{\hbar\omega_\nu} &= K_{yx}(t, t').
\end{aligned} \tag{14}$$

The validity of the fluctuation-dissipation relations means that we have properly identified the dissipative terms in the non-Markovian dynamical equations of motion. The quantum fluctuation-dissipation relations differ from the classical ones and are reduced to them in the limit of high temperature.

## B. Solution of Non-Markovian Langevin equations

In order to solve the equations of motion (8) for the collective variables, we apply the Laplace transformation. It significantly simplifies the solution of the problem. After the Laplace transformation, the equations of motion read

$$\begin{aligned}
x(s)s &= x(0) + \frac{\pi_x(s)}{m_x}, \quad y(s)s = y(0) + \frac{\pi_y(s)}{m_y}, \\
\pi_x(s)s + \frac{\pi_x(s)}{m_x}(K_{xx}(s) + K_{xy}(s)) &= \pi_x(0) + \omega_{cy}\pi_y(s) - \frac{1}{s}eE_x + F_x(s), \\
\pi_y(s)s + \frac{\pi_y(s)}{m_y}(K_{yy}(s) + K_{yx}(s)) &= \pi_y(0) - \omega_{cx}\pi_x(s) + F_y(s).
\end{aligned} \tag{15}$$

Here,  $K_{xx}(s)$ ,  $K_{yy}(s)$ ,  $K_{xy}(s)$ ,  $K_{yx}(s)$  and  $F_x(s)$ ,  $F_y(s)$  are the Laplace transforms of the dissipative kernels and random forces, respectively. To solve these equations, one should

find the roots of the determinant

$$D = s(m_x m_y \omega_c^2 + [K_{xx}(s) + K_{xy}(s) + m_x s][K_{yy}(s) + K_{yx}(s) + m_y s]) = 0. \quad (16)$$

The explicit solutions for the originals are

$$\begin{aligned} x(t) &= x(0) + A_1(t)\pi_x(0) + A_2(t)\pi_y(0) - A_3(t)eE_x + I_x(t) + I'_x(t), \\ y(t) &= y(0) + B_1(t)\pi_y(0) - B_2(t)\pi_x(0) + B_3(t)eE_x - I_y(t) + I'_y(t), \\ \pi_x(t) &= C_1(t)\pi_x(0) + C_2(t)\pi_y(0) - C_3(t)eE_x + I_{\pi_x}(t) + I'_{\pi_x}(t), \\ \pi_y(t) &= D_1(t)\pi_y(0) - D_2(t)\pi_x(0) + D_3(t)eE_x - I_{\pi_y}(t) + I'_{\pi_y}(t), \end{aligned} \quad (17)$$

where

$$\begin{aligned} I_x(t) &= \int_0^t A_1(\tau)F_x(t-\tau)d\tau, & I'_x(t) &= \int_0^t A_2(\tau)F_y(t-\tau)d\tau, \\ I_y(t) &= \int_0^t B_2(\tau)F_x(t-\tau)d\tau, & I'_y(t) &= \int_0^t B_1(\tau)F_y(t-\tau)d\tau, \\ I_{\pi_x}(t) &= \int_0^t C_1(\tau)F_x(t-\tau)d\tau, & I'_{\pi_x}(t) &= \int_0^t C_2(\tau)F_y(t-\tau)d\tau, \\ I_{\pi_y}(t) &= \int_0^t D_2(\tau)F_x(t-\tau)d\tau, & I'_{\pi_y}(t) &= \int_0^t D_1(\tau)F_y(t-\tau)d\tau \end{aligned}$$

with the following time-dependent coefficients:

$$\begin{aligned} A_1(t) &= \hat{L}^{-1} \left[ \frac{K_{yy}(s) + K_{yx}(s) + m_y s}{D} \right] = B_1(t)|_{x \leftrightarrow y}, \\ A_2(t) &= m_y \omega_{cy} \hat{L}^{-1} \left[ \frac{1}{D} \right] = B_2(t)|_{x \leftrightarrow y}, \\ A_3(t) &= \hat{L}^{-1} \left[ \frac{K_{yy}(s) + K_{yx}(s) + m_y s}{sD} \right], & B_3(t) &= m_x \omega_{cx} \hat{L}^{-1} \left[ \frac{1}{sD} \right], \\ C_1(t) &= m_x \hat{L}^{-1} \left[ \frac{s(K_{yy}(s) + K_{yx}(s) + m_y s)}{D} \right] = D_1(t)|_{x \leftrightarrow y}, \\ C_2(t) &= m_x m_y \omega_{cy} \hat{L}^{-1} \left[ \frac{s}{D} \right] = D_2(t)|_{x \leftrightarrow y}, \\ C_3(t) &= m_x \hat{L}^{-1} \left[ \frac{K_{yy}(s) + K_{yx}(s) + m_y s}{D} \right], & D_3(t) &= m_x m_y \omega_{cx} \hat{L}^{-1} \left[ \frac{1}{D} \right]. \end{aligned} \quad (18)$$

Here,  $\hat{L}^{-1}$  denotes the inverse Laplace transformation. The exact solutions of  $x(t)$ ,  $y(t)$ ,  $\pi_x(t)$ , and  $\pi_y(t)$  in terms of roots  $s_i$  are given by the residue theorem.

For the system with linear coupling in coordinate, the coupling term is written as

$$H_{cb} = \sum_{\nu} (\alpha_{\nu} x + \beta_{\nu} y)(b_{\nu}^+ + b_{\nu}) + \sum_{\nu} \frac{1}{\hbar \omega_{\nu}} (\alpha_{\nu} x + \beta_{\nu} y)^2, \quad (19)$$



where  $\alpha_\nu$  and  $\beta_\nu$  are the real coupling constants. Here, we again introduce the counter term which depends on the coordinates of collective system and is treated as a part of the potential. The operators of random forces and dissipative kernels in Eqs. (8) are

$$F_x(t) = - \sum_\nu \alpha_\nu (f_\nu^+ + f_\nu), \quad F_y(t) = - \sum_\nu \beta_\nu (f_\nu^+ + f_\nu)$$

and

$$\begin{aligned} K_{xx}(t - \tau) &= \sum_\nu \frac{2\alpha_\nu^2}{\hbar\omega_\nu} \cos(\omega_\nu[t - \tau]), \\ K_{yy}(t - \tau) &= \sum_\nu \frac{2\beta_\nu^2}{\hbar\omega_\nu} \cos(\omega_\nu[t - \tau]), \end{aligned} \quad (20)$$

respectively. We assume that there are no correlations between  $F_x^\nu$  and  $F_y^\nu$ , so that  $K_{xy} = K_{yx} = 0$ . If the coupling constants  $\alpha_\nu$  and  $\beta_\nu$  depend on magnetic field, then the dissipative kernels  $K_{xx}$  and  $K_{yy}$  are the functions of  $B$ .

It is convenient to introduce the spectral density  $D_\omega$  of the heat bath excitations to replace the sum over different oscillators by an integral over the frequency:  $\sum_\nu \dots \rightarrow \int_0^\infty d\omega D_\omega \dots$ . This replacement is accompanied by the following replacements:  $\alpha_\nu \rightarrow \alpha_\omega$ ,  $\beta_\nu \rightarrow \beta_\omega$ ,  $\omega_\nu \rightarrow \omega$ , and  $n_\nu \rightarrow n_\omega$ . Let us consider the following spectral functions [28]

$$D_\omega \frac{|\alpha_\omega|^2}{\hbar\omega} = \frac{\alpha^2}{\pi} \frac{\gamma^2}{\gamma^2 + \omega^2}, \quad D_\omega \frac{|\beta_\omega|^2}{\hbar\omega} = \frac{\beta^2}{\pi} \frac{\gamma^2}{\gamma^2 + \omega^2}, \quad (21)$$

where the memory time  $\gamma^{-1}$  of the dissipation is inverse to the phonon bandwidth of the heat bath excitations which are coupled to a quantum particle. This is the Ohmic dissipation with the Lorentian cutoff (Drude dissipation) [20–25, 28, 36].

Using the spectral functions (21), we obtain the dissipative kernels and their Laplace transforms in the convenient form

$$\begin{aligned} K_{xx}(t) &= m_x \lambda_x \gamma e^{-\gamma|t|}, & K_{yy}(t) &= m_y \lambda_y \gamma e^{-\gamma|t|}, \\ K_{xx}(s) &= \frac{m_x \lambda_x \gamma}{s + \gamma}, & K_{yy}(s) &= \frac{m_y \lambda_y \gamma}{s + \gamma}, \end{aligned} \quad (22)$$

where

$$\lambda_x = \hbar\alpha^2 = \frac{1}{m_x} \int_0^\infty K_{xx}(t - \tau) d\tau, \quad \lambda_y = \hbar\beta^2 = \frac{1}{m_y} \int_0^\infty K_{yy}(t - \tau) d\tau$$

are the friction coefficients in the Markovian limit. So, the solutions for the collective variables (17) include the following time-dependent coefficients:

$$\begin{aligned}
A_1(t) &= \dot{A}_3(t), & A_2(t) &= \dot{B}_3(t)|_{x \leftrightarrow y}, \\
A_3(t) &= \frac{1}{m_x} \left( \frac{\lambda_y}{\lambda_x \lambda_y + \omega_c^2} t + \frac{\omega_c^2(\gamma - \lambda_y) - \lambda_y^2(\gamma - \lambda_x)}{\gamma(\lambda_x \lambda_y + \omega_{cx} \omega_{cy})^2} \right. \\
&\quad \left. + \sum_{i=1}^4 \frac{b_i e^{s_i t} (\gamma + s_i) (\gamma \lambda_y + s_i (\gamma + s_i))}{s_i^2} \right), \\
B_1(t) &= \dot{A}_3(t)|_{x \leftrightarrow y}, & B_2(t) &= \dot{B}_3(t), \\
B_3(t) &= \frac{\omega_{cx}}{m_y} \left( \frac{t}{\lambda_x \lambda_y + \omega_{cx} \omega_{cy}} + \frac{2\lambda_x \lambda_y - \gamma(\lambda_x + \lambda_y)}{\gamma(\lambda_x \lambda_y + \omega_{cx} \omega_{cy})^2} + \sum_{i=1}^4 \frac{b_i e^{s_i t} (\gamma + s_i)^2}{s_i^2} \right), \\
C_1(t) &= m_x \ddot{A}_3(t), & C_2(t) &= m_x \ddot{B}_3(t), & C_3(t) &= m_x \dot{A}_3(t), \\
D_1(t) &= C_1(t)|_{x \leftrightarrow y}, & D_2(t) &= m_y \ddot{B}_3(t), & D_3(t) &= m_y \dot{B}_3(t),
\end{aligned} \tag{23}$$

where  $b_i = [\prod_{j \neq i} (s_i - s_j)]^{-1}$  with  $i, j = 1, 2, 3, 4$  and  $s_i$  are the roots of the equation

$$\gamma \lambda_x [\gamma \lambda_y + s(\gamma + s)] + (\gamma + s)(s[s^2 + \omega_c^2] + \gamma[\omega_c^2 + s(\lambda_y + s)]) = 0. \tag{24}$$

### C. Galvano-magnetic effects

In order to determine the transport coefficients, we use Eqs. (17). Averaging them over the whole system and by differentiating in  $t$ , we obtain the system of equations for the first moments

$$\begin{aligned}
\langle \dot{x}(t) \rangle &= \frac{\langle \pi_x(t) \rangle}{m_x}, & \langle \dot{y}(t) \rangle &= \frac{\langle \pi_y(t) \rangle}{m_y}, \\
\langle \dot{\pi}_x(t) \rangle &= \tilde{\omega}_{cy}(t) \langle \pi_y(t) \rangle - \lambda_{\pi_x}(t) \langle \pi_x(t) \rangle - e \tilde{E}_{xx}(t), \\
\langle \dot{\pi}_y(t) \rangle &= -\tilde{\omega}_{cx}(t) \langle \pi_x(t) \rangle - \lambda_{\pi_y}(t) \langle \pi_y(t) \rangle - e \tilde{E}_{xy}(t),
\end{aligned} \tag{25}$$

with the friction coefficients

$$\begin{aligned}
\lambda_{\pi_x}(t) &= -\frac{D_1(t) \dot{C}_1(t) + D_2(t) \dot{C}_2(t)}{C_1(t) D_1(t) + C_2(t) D_2(t)}, \\
\lambda_{\pi_y}(t) &= -\frac{C_1(t) \dot{D}_1(t) + C_2(t) \dot{D}_2(t)}{C_1(t) D_1(t) + C_2(t) D_2(t)},
\end{aligned} \tag{26}$$

and renormalized cyclotron frequencies

$$\begin{aligned}
\tilde{\omega}_{cx}(t) &= \frac{D_1(t) \dot{D}_2(t) - D_2(t) \dot{D}_1(t)}{C_1(t) D_1(t) + C_2(t) D_2(t)}, \\
\tilde{\omega}_{cy}(t) &= \frac{C_1(t) \dot{C}_2(t) - C_2(t) \dot{C}_1(t)}{C_1(t) D_1(t) + C_2(t) D_2(t)},
\end{aligned} \tag{27}$$

while the components of the electric field read:

$$\begin{aligned}\tilde{E}_{xx}(t) &= E_x[D_3(t)\tilde{\omega}_{cy}(t) + C_3(t)\lambda_{\pi_x}(t) + \dot{C}_3(t)], \\ \tilde{E}_{xy}(t) &= E_x[C_3(t)\tilde{\omega}_{cx}(t) - D_3(t)\lambda_{\pi_y}(t) - \dot{D}_3(t)].\end{aligned}\quad (28)$$

As seen, the dynamics is governed by the non-stationary coefficients. As found, the external magnetic field generates the flow of charge carriers and electric field in the cross direction (the classical Hall effect). It should be noted that the cross component  $\tilde{E}_{xy}(t)$  of the electric field is initially absent and appears during the non-Markovian evolution of the collective subsystem.

Let us consider the magneto-transport process in the two-dimensional system with current density defined as [1–3]

$$J_i = \sum_{j=1}^2 \sigma_{ij}(\mathbf{B}) E_j. \quad (29)$$

Here,  $\sigma_{ij}(\mathbf{B})$  is the electric conductivity tensor which depends on the magnitude and direction of the magnetic field  $\mathbf{B}$ . One can also define the current density by using the expression for the collective momentum (17) and the fact that  $\mathbf{J} = -ne\dot{\mathbf{R}}$  because

$$J_x = \frac{ne^2}{m_j} C_3(t) E_x(t), \quad J_y = -\frac{ne^2}{m_y} D_3(t) E_x(t). \quad (30)$$

If we change the direction of the external electric field  $\vec{E}(E_x, 0, 0)$  to  $\vec{E}(0, E_y, 0)$ , the expression for the current density (30) change to

$$J_x = \frac{ne^2}{m_x} \tilde{D}_3(t) E_y(t), \quad J_y = \frac{ne^2}{m_y} \tilde{C}_3(t) E_y(t), \quad (31)$$

where

$$\tilde{C}_3(t) = m_y L^{-1} \left[ \frac{K_{xx}(s) + K_{xy}(s) + m_x s}{D} \right], \quad \tilde{D}_3(t) = m_x m_y \omega_{cy} L^{-1} \left[ \frac{1}{D} \right].$$

Comparing (35) with (30) and (31), one can write the expression for conductivity tensor at time  $t = \tau$

$$\sigma(\tau) = ne^2 \begin{pmatrix} \frac{C_3(\tau)}{m_x} & -\frac{D_3(\tau)}{m_y} \\ \frac{\tilde{D}_3(\tau)}{m_x} & \frac{\tilde{C}_3(\tau)}{m_y} \end{pmatrix}, \quad (32)$$

while its inverse transformation yields the specific resistance tensor

$$\rho(\tau) = \frac{1}{ne^2[C_3(\tau)\tilde{C}_3(\tau) + D_3(\tau)\tilde{D}_3(\tau)]} \begin{pmatrix} m_x \tilde{C}_3(\tau) & m_x D_3(\tau) \\ -m_y \tilde{D}_3(\tau) & m_y C_3(\tau) \end{pmatrix}. \quad (33)$$

The non-diagonal elements of the specific magneto-resistance tensor have the meaning of the Hall resistance

$$\rho_H(\tau) = \frac{m_x D_3(\tau)}{ne^2[C_3(\tau)\tilde{C}_3(\tau) + D_3(\tau)\tilde{D}_3(\tau)]} = \frac{m_y \tilde{D}_3(\tau)}{ne^2[C_3(\tau)\tilde{C}_3(\tau) + D_3(\tau)\tilde{D}_3(\tau)]}. \quad (34)$$

In the case of two charge carriers, the model is generalized in Appendix A.

#### D. The main assumptions of the model

Here, we list the main assumptions of the model which allow us to proceed with the calculations for real systems. We suppose that in each collision the charge carriers lose their ordered motion and their velocities vanish. As in the kinetic theory of gases, in our model we assume that the lengths and times  $t = \tau$  of free path are the same for all charge carriers and all collisions. So, we introduce the time limit  $t = \tau$  in the conductivity tensor (32) or resistance tensor (33). In our model there are three different characteristic times describing the dynamics of charge carriers: 1) the relaxation time  $\tau_r = \lambda^{-1}$  ( $\lambda = \lambda_x = \lambda_y$ ), 2) the average time between two collisions  $\tau$ , and 3) the memory time  $\gamma^{-1}$  of the heat bath excitations. The values of  $\tau_r$  and  $\tau$  are related with one-body (mean-field) and two-body effects (dissipations). So, by introducing the time parameter  $\tau$ , we take effectively into consideration the two-body collisions of charge carriers. The mean free time  $\tau$  is related to the thermodynamic equilibrium properties of the material, whereas the relaxation time  $\tau_r$  relates to the thermal and electrical transport properties (see Fig. 1). The relaxation time  $\tau_r$  of electrons is the characteristic time for a distribution of charge carriers in a solid to approach or "relax" to equilibrium after the disturbance is removed. A familiar example is the relaxation of current to zero equilibrium value after the external electric field is turned off. Highly conductive materials have relatively long relaxation and free motion times. At  $\tau \gg \tau_r$ , the one-body (mean-field) dissipation dominates. If these times are comparable, then the process has a transitional behavior. Note that in general the values of  $\tau_r$  and  $\tau$  depend on temperature  $T$  and the strength of magnetic field  $B$ .

#### E. Axial symmetric system

One can obtain clearer physical picture of the process, if the space-symmetric system is considered. In this system  $m_x = m_y = m$ ,  $\lambda_x = \lambda_y = \lambda$ , and  $\omega_{cx} = \omega_{cy} = \omega_c$ . So, Eqs. (24),

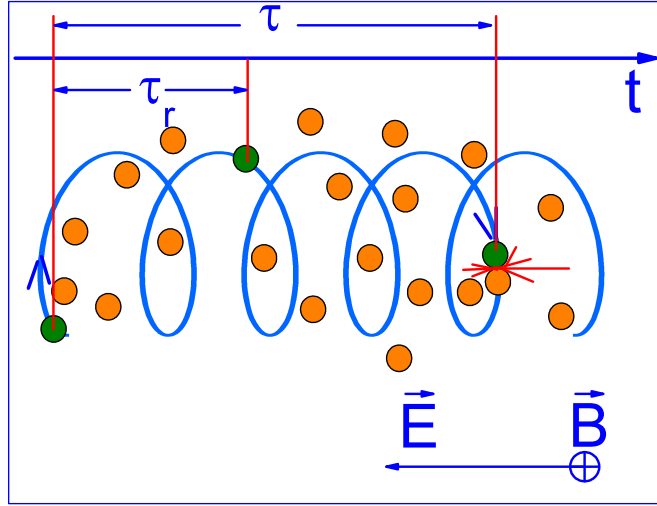


FIG. 1: Schematic presentation of the scattering process and different time scales in a two-dimensional magneto-transport.

which defines the poles, is simplified:

$$(s^2 + \omega_c^2)(\gamma + s)^2 + 2\gamma\lambda s(\gamma + s) + \lambda^2\gamma^2 = 0. \quad (35)$$

This equation has the roots

$$\begin{aligned} s_1 &= -\frac{1}{2} \left( \gamma + i\omega_c + \sqrt{(\gamma - i\omega_c)^2 - 4\gamma\lambda} \right), & s_2 &= s_1^*, \\ s_3 &= -\frac{1}{2} \left( \gamma + i\omega_c - \sqrt{(\gamma - i\omega_c)^2 - 4\gamma\lambda} \right), & s_4 &= s_3^*. \end{aligned}$$

In order to split the real and imaginary parts of the roots, we expand them up to the first order in  $\lambda/\gamma$ :

$$\begin{aligned} s_1 &= -\frac{\lambda\gamma^2}{\gamma^2 + \omega_c^2} - i\frac{\omega_c^2 + \gamma^2 + \lambda\gamma}{\gamma^2 + \omega_c^2}\omega_c, \\ s_3 &= -\gamma\frac{\gamma^2 + \omega_c^2 - \gamma\lambda}{\gamma^2 + \omega_c^2} + i\frac{\lambda\gamma\omega_c}{\gamma^2 + \omega_c^2}. \end{aligned}$$

In this approximation, the components of conductivity (32) at  $t = \tau$  are

$$\begin{aligned}
\sigma_{xx}(\tau) &= \frac{\sigma_{xx0}}{1 + (\omega_c \tau_r)^2} \\
&\quad - \frac{\sigma_{xx0}}{\sqrt{1 + (\omega_c \tau_r)^2}} \exp\left[-\frac{\gamma^2}{\gamma^2 + \omega_c^2} \frac{\tau}{\tau_r}\right] \cos\left[\frac{(\gamma^2 + \gamma/\tau_r + \omega_c^2)\omega_c \tau}{\gamma^2 + \omega_c^2} + \arctan\left(\frac{1}{\omega_c \tau_r}\right)\right], \\
\sigma_{xy}(\tau) &= \frac{\sigma_{xx0} \omega_c \tau_r}{1 + (\omega_c \tau_r)^2} \\
&\quad - \frac{\sigma_{xx0}}{\sqrt{1 + (\omega_c \tau_r)^2}} \exp\left[-\frac{\gamma^2}{\gamma^2 + \omega_c^2} \frac{\tau}{\tau_r}\right] \cos\left[\frac{(\gamma^2 + \gamma/\tau_r + \omega_c^2)\omega_c \tau}{\gamma^2 + \omega_c^2} - \arctan(\omega_c \tau_r)\right]. \quad (36)
\end{aligned}$$

As seen, the expressions for macroscopically observable values such as the cross and longitudinal components of conductivity (resistance) contain the non-oscillatory and oscillatory parts. In very strong magnetic fields, when the cyclotron frequency is much larger than the friction of the system  $\omega_c \gg \tau_r^{-1}$ , the longitudinal and transverse components of conductivity oscillate in antiphase. Depending on the ratio between  $\tau_r$  and  $\tau$ , the oscillatory or non-oscillatory term of (36) has a major role. At  $\tau \gg \tau_r$  or  $\tau \rightarrow \infty$ , the oscillatory term vanishes and we obtain the Drude conductivity

$$\sigma = \frac{\sigma_{xx0}}{1 + (\omega_c \tau_r)^2} \begin{pmatrix} 1 & -\omega_c \tau_r \\ \omega_c \tau_r & 1 \end{pmatrix}, \quad (37)$$

where

$$\sigma_{xx0} = \frac{ne^2 \tau_r}{m}$$

is the Drude conductivity at  $B = 0$ . As seen, the conductivity (36) differs from the Drude one at  $B \neq 0$  by additional oscillatory term.

## F. Thermomagnetic effects

Here, we assume that the electric and thermal currents are carried by the same particles and find the relation between the electric and thermal conductivities. If the electric energy gradient  $eE$  in the Hamiltonian (2) is substituted by the temperature gradient  $\frac{dT}{dx}$  (the temperature is in energy units), the generating force of particle motion is changed from the electric to thermal potential, giving rise to the thermomagnetic effects. Taking into consideration the expression for the heat flux

$$\mathbf{Q} = n\varepsilon_{kin} \dot{\mathbf{R}},$$

and following the procedure of subsection II.C, we find the expressions for the components of thermal conductivity tensor

$$\chi(\tau) = \frac{1}{e^2} \varepsilon_{kin}(\tau) \sigma(\tau), \quad (38)$$

where  $\varepsilon_{kin}$  is the kinetic energy of charge carriers. The kinetic energy is defined through the variances  $\Sigma_{\pi_x \pi_x}$  and  $\Sigma_{\pi_y \pi_y}$  (Appendix B) and mean values  $\langle \pi_x \rangle$  and  $\langle \pi_y \rangle$ . In the quasi-equilibrium high temperature limit ( $\tau \rightarrow \infty$ ), the kinetic energy

$$\varepsilon_{kin}(\infty) = T \quad (39)$$

is defined by the equipartition theorem (the equilibrium variances  $\Sigma_{\pi_x \pi_x}(\infty) = m_x T$  and  $\Sigma_{\pi_y \pi_y}(\infty) = m_y T$ ). Finally, one can rederive the classical Wiedemann-Franz law [1–3]

$$L = \frac{\chi}{T\sigma} = \frac{1}{e^2} = const,$$

where  $L$  is the Lorentz number which reflects the fact that the ability of the carriers to carry a charge is the same as to transport heat.

### III. CALCULATED RESULTS AND DISCUSSIONS

In the calculations we set  $\lambda = \lambda_x = \lambda_y$  (or  $\lambda_\pi = \lambda_{\pi_x} = \lambda_{\pi_y}$ ) and  $m = m_x = m_y$  (or  $\omega_c = \omega_{cx} = \omega_{cy}$ ). In order to turn to the observable values, all parameters  $\tau^{-1}$ ,  $\tau_r^{-1}$ ,  $\omega_c$ , and  $\gamma$  in the expressions are multiplied by  $\frac{m}{e}$ :

$$\begin{aligned} \tau^{-1} &\rightarrow \frac{m}{e} \tau^{-1}, \\ \tau_r^{-1} &\rightarrow \frac{m}{e} \tau_r^{-1} = \mu^{-1}, \\ \omega_c &\rightarrow \frac{m}{e} \omega_c = B, \\ \gamma &\rightarrow \frac{m}{e} \gamma = \Gamma. \end{aligned} \quad (40)$$

As a result, instead of the friction coefficient  $\lambda$ , cyclotron frequency  $\omega_c$ , and inverse response time  $\gamma$  of the system we have the inverse reciprocal mobility  $\mu^{-1}$  of charge carriers, intensity of the magnetic field  $B$ , and new parameter  $\Gamma$  connected to the memory time. The mobility of a charge carrier  $\mu_0 = \mu(B = 0)$  in the absence of magnetic field is the measurable value. The value of  $B$  is set by the experimental condition.

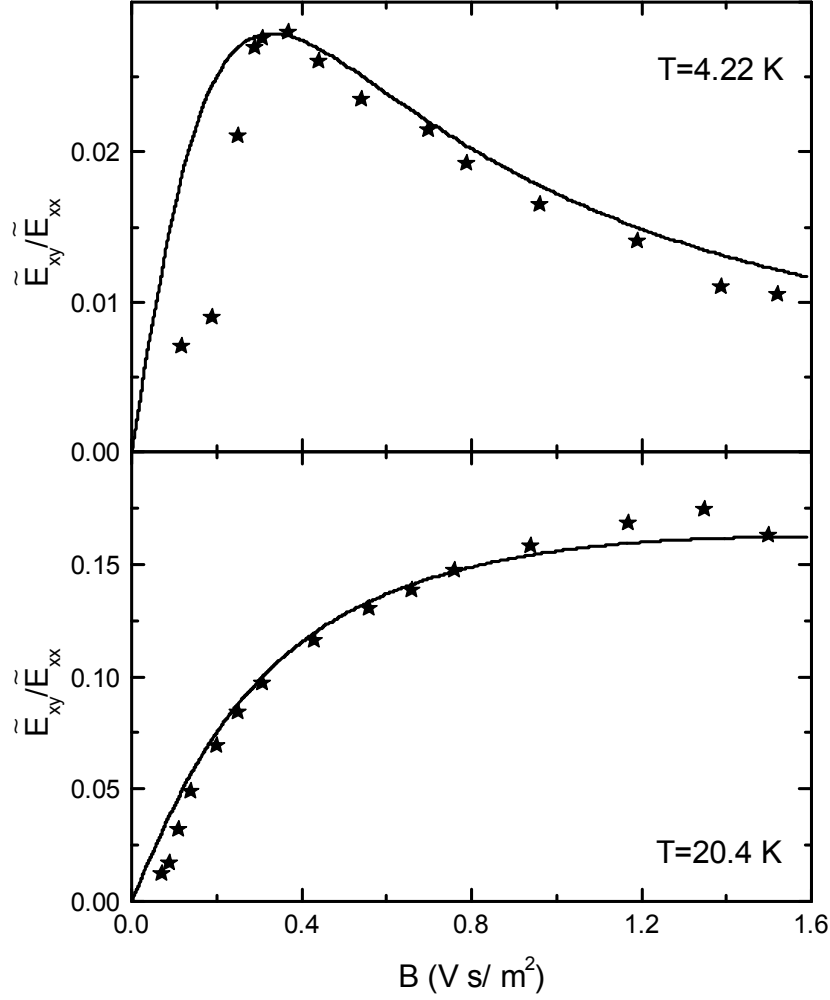


FIG. 2: The experimental [4] (symbols) and theoretical dependencies (lines) of the tangent of the Hall angle on magnetic field  $B$  for zinc at temperatures  $T$  indicated.

In addition, one can also study the magnetic moment of the system. It should be noted that in our model the influence of the magnetic field on the coupling between quantum particle and heat-bath is neglected. The impact of magnetic field is entered into the dissipative kernels. However, there are solids with constant resistance in the wide spectrum of magnetic field. Their properties can be described by neglecting the effect of magnetic field



on the coupling term.

### A. Classical Hall effect

The classical case corresponds  $\tau \gg \tau_r$  or  $\tau \rightarrow \infty$ . To demonstrate the capabilities of the model, we calculate the tangent of the Hall angle,  $\tan[\Theta_H] = \tilde{E}_{xy}(\infty)/\tilde{E}_{xx}(\infty)$ , for the sample of Zn settled in the increasing external magnetic field at two temperatures. Many experiments were performed to measure this value in several materials. We choose Zn [4] because it has one type of charge carriers, and consequently, the technique of implementation of the model can be easily understood. The calculated and experimental characteristics of Zn are listed in Table I. The calculations performed with the values of mobility  $\mu_0$  at  $B = 0$  are in a good agreement with the experimental data (Fig. 2), especially at high strength of magnetic field.

TABLE I: Experimental (asterisks) [4] and theoretical characteristics of Zn at two temperatures. The value of  $B_{max}^*$  corresponds to the position of the maximum of experimental non-diagonal component of electric field as a function of magnetic field.

Temperature*, $T$ (K)	Resistance*, $\rho_{xx}$ , $\times 10^{-11}$ ( $\Omega \cdot \text{m}$ )	Mobility, $\mu_0$ ( $\text{m}^2 / \text{V} \cdot \text{s}$ )	$\Gamma = B_{max}^*$ , (Tesla)	Max. Hall angle*, $\Theta_H$
4.22	2.6555	50.25	0.37	$1.6^\circ$
20.4	35.595	1.1	1.35	$9.37^\circ$

### B. Integer Hall effect

The IQHE has been observed in the heterostructure GaAs-Al<sub>0.3</sub>Ga<sub>0.7</sub>As at the low temperature of  $T = 50$  mK [8]. According to the experiment, the concentration of the artificially prepared two-dimensional sample GaAs-Al<sub>0.3</sub>Ga<sub>0.7</sub>As is  $n = 3.7 \cdot 10^{15} \text{ m}^{-2}$ . There are large intervals of  $B$  where the longitudinal conductivity has its minimum, while the Hall conductivity is quantized with immense precision in integer multiples of  $e^2/(2\pi\hbar)$ . The calculated components of the resistivity tensor are shown in Fig. 3 for wide range of magnetic field.

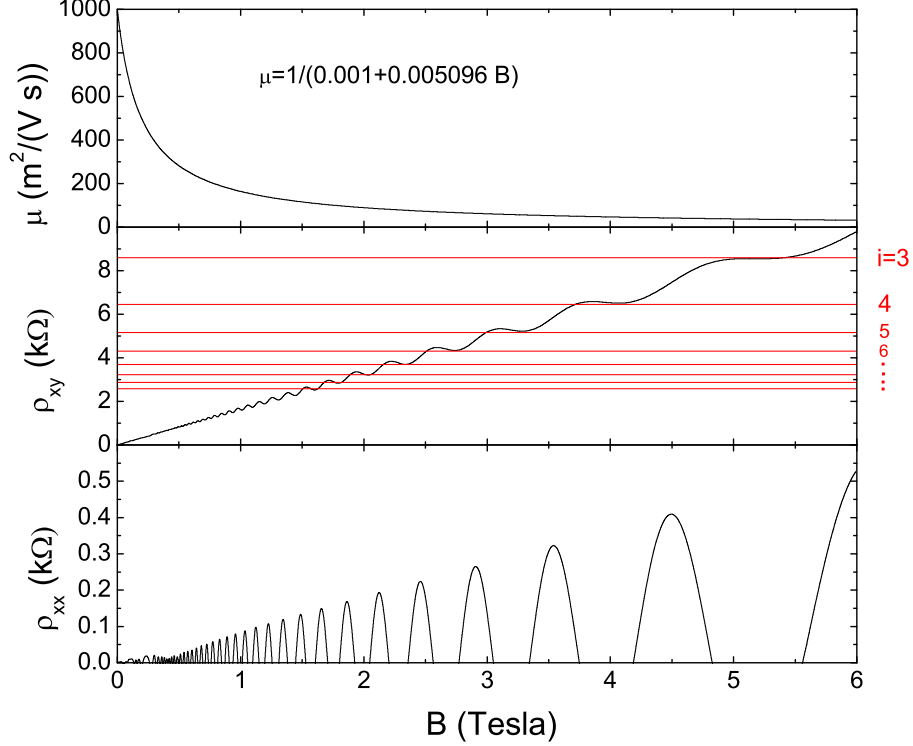


FIG. 3: Theoretical plots of the components of resistivity tensor and mobility of charge carriers in GaAs-Al<sub>0.3</sub>Ga<sub>0.7</sub>As at  $T = 50$  mK. The experimental concentration,  $n = 3.7 \cdot 10^{15} \text{ m}^{-2}$ , is from Ref. [8] and the mobility has the functional form  $\mu(B) = 1/(0.001 + 0.005096B)$  indicated on the plot. The ratio of mean collision time per relaxation time is set to be  $\frac{\tau}{\tau_r} = 2$ , and  $\Gamma = 100/\mu_0$ .

The observed increase of the width of plateau in  $\rho_{xy}$  with the field is explained by the decrease of the mean collision time of charge carriers. The external magnetic field effects the coupling between the collective system and heat-bath. This coupling linearly rises with the magnetic field which induces the reciprocal decrease of  $\tau_r$ . Such a decrease in relaxation time effectively changes the mobility of charge carriers (Fig. 3). The drastic decrease of mobility can be attributed to the effect of localization under the influence of magnetic field. For the formation of the step-wise nature of  $\rho_{xy}$ , the ratio  $\tau/\tau_r$  is required to be constant at whole magnetic field spectrum. Thus, both the mean collision time and relaxation time fall down inversely with increasing magnetic field, as in the experiment [1]. However, the ratio between them remains constant. As seen in Fig. 3, in the region between two plateaus for  $\rho_{xy}$  the longitudinal resistivity has the maximum, while at the center of plateau it is minimal. This phenomenon is explained by the  $\pi/2$  phase shift in the oscillations of  $\rho_{xx}$  and

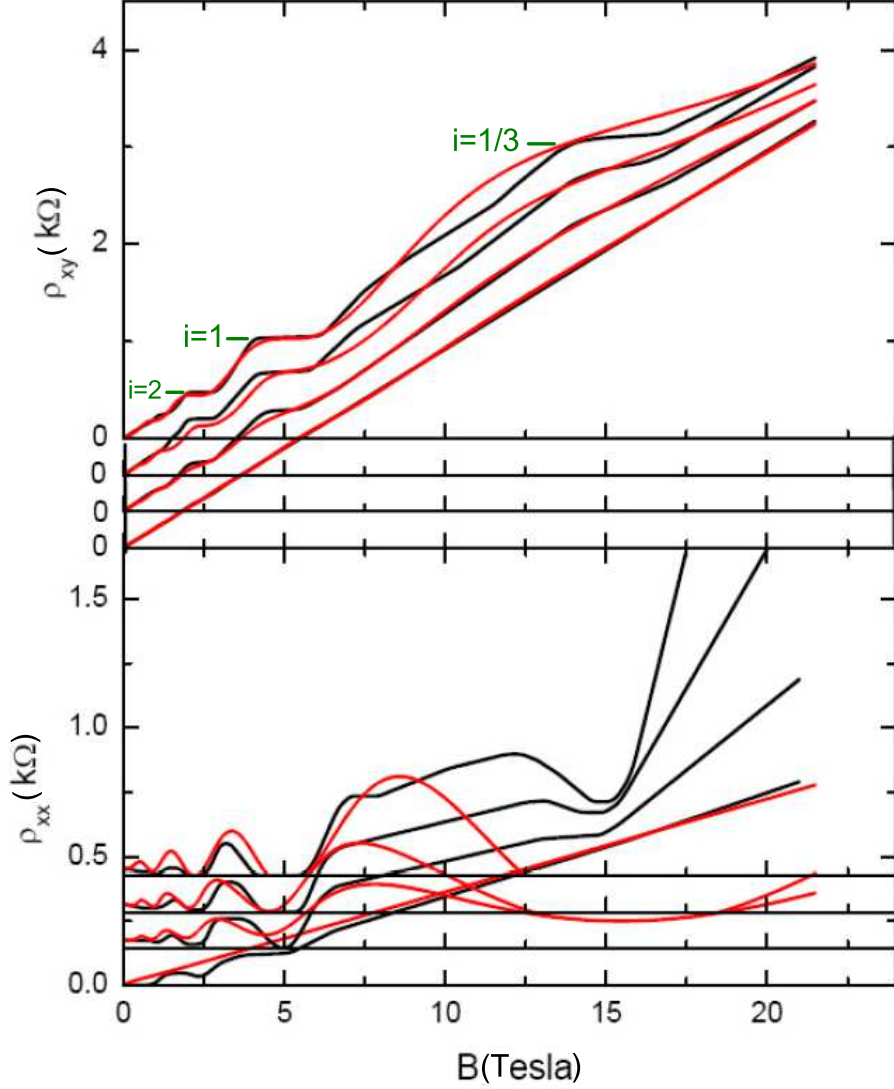


FIG. 4: The experimental (black) [9] and theoretical (red) curves of magnetic field dependencies of the components of resistivity tensor at different temperatures  $T=0.48, 1.00, 1.65, 4.15$  K in the order from top to bottom.

$\rho_{xy}$  which is clearly visible in the approximate formulas for the axial symmetric system at very strong magnetic fields ( $\omega_c \tau_r \gg 1$ ):

$$\frac{\rho_{xx}}{\rho_{xx0}} = 1 - \mu B \exp \left[ -\frac{\Gamma^2}{\Gamma^2 + B^2} \frac{\tau}{\tau_r} \right] \cos \left[ \frac{(\Gamma^2 + \Gamma/\mu + B^2)(e/m)\tau B}{\Gamma^2 + B^2} \right],$$

$$\frac{\rho_{xy}}{\rho_{xx0}} = \mu B \left( 1 - \exp \left[ -\frac{\Gamma^2}{\Gamma^2 + B^2} \frac{\tau}{\tau_r} \right] \sin \left[ \frac{(\Gamma^2 + \Gamma/\mu + B^2)(e/m)\tau B}{\Gamma^2 + B^2} \right] \right),$$

where  $\rho_{xx0} = 1/\sigma_{xx0}$ .

### C. Fractional Hall effect

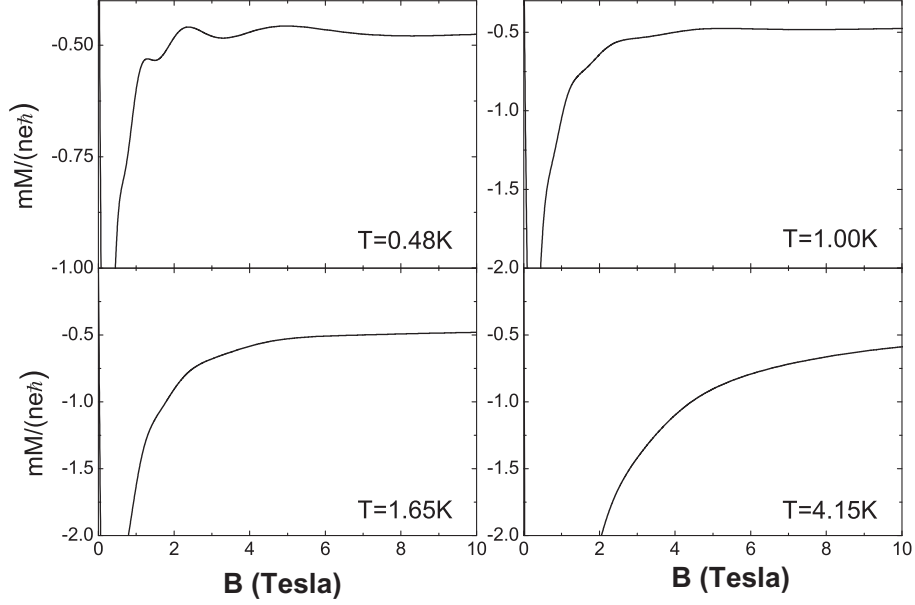


FIG. 5: The calculated magnetic moment as a function of magnetic field at indicated temperatures.

The Hall plateau at strong magnetic field has been discovered in Ref. [9] (Fig. 4) and corresponds to the fractional value of the filling factor  $i = 1/3$ . The experiment has been carried out at four temperatures below the helium temperature for the sample of GaAs- $\text{Al}_{0.3}\text{Ga}_{0.7}\text{As}$  with the 2D concentration  $n = 1.23 \cdot 10^{15} \text{ m}^{-2}$  and carrier mobility  $\mu_0 = 9 \text{ m}^2/(\text{V} \cdot \text{s})$ . The step-wise appearance of the Hall resistivity becomes smoother with increasing temperature. The purity of the sample is so high that the electrons move ballistically, i.e. without scattering against impurity atoms, over relatively long distances. In our calculations (Fig. 4), we take the experimental values of mobility  $\mu_0$  and 2D concentration  $n$  and  $\Gamma = 100/\mu_0$  (Table II). As in the case of the integer Hall effect, the relaxation time and mean collision time of charge carriers decrease inversely with increasing magnetic field and their ratio remains constant (Table II).

We also calculate the magnetic moment  $M(\tau) = \frac{neL_z(\tau)}{2m}$ , where

$$\begin{aligned}
 L_z(\tau) &= \langle x(\tau)\pi_y(\tau) - y(\tau)\pi_x(\tau) \rangle \\
 &= \frac{m\hbar\gamma^2}{\pi} \int_0^\infty \int_0^\tau \int_0^\tau \frac{d\omega dt dt' \omega \coth\left[\frac{\hbar\omega}{2T}\right] \cos(\omega[t-t'])}{\omega^2 + \gamma^2} \\
 &\quad \times \{ \lambda_x [B_2(t)C_1(t') - A_1(t)D_2(t')] + \lambda_y [A_2(t)D_1(t') - B_1(t)C_2(t')] \} \quad (41)
 \end{aligned}$$

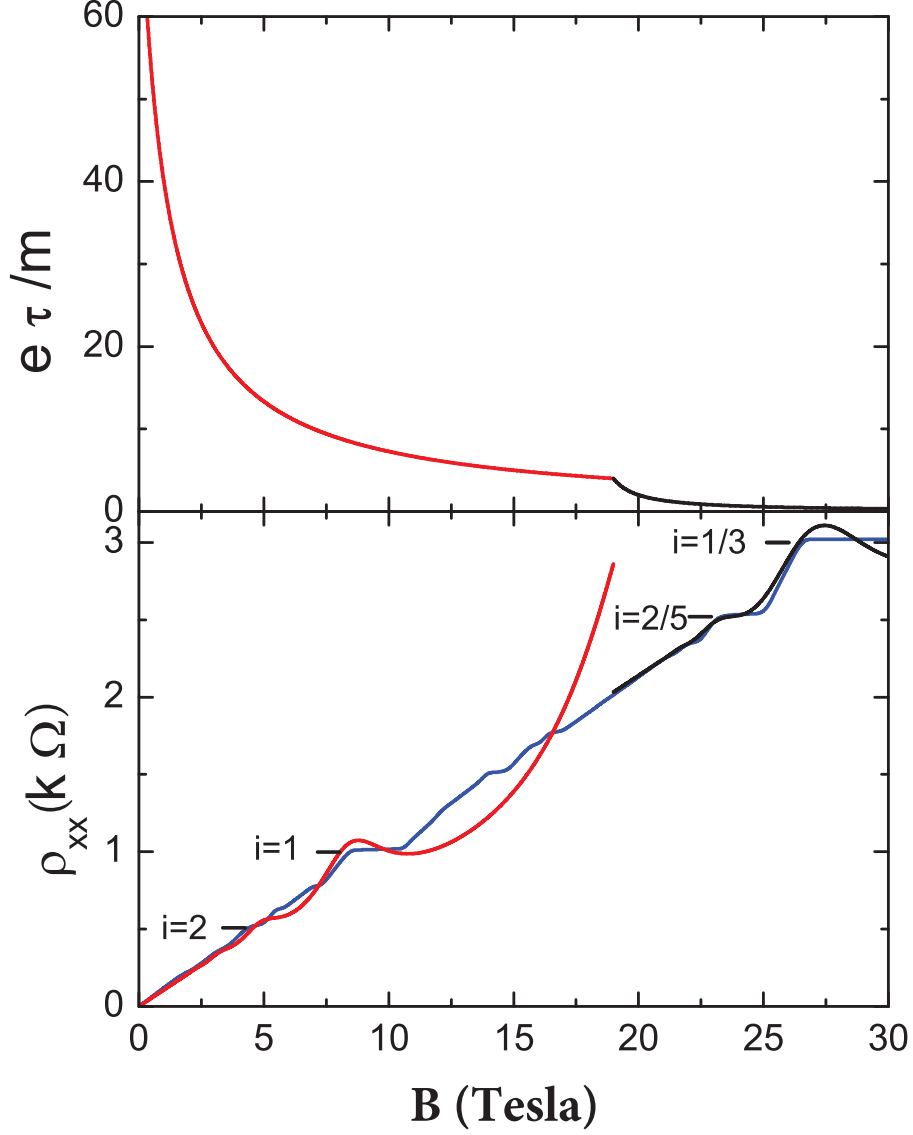


FIG. 6: The calculated dependence of transverse component of resistivity and the mean free time on magnetic field. The blue line corresponds to the experiment [10].

is the  $z$ -component of angular momentum. The calculations were performed with the parameters from Table II. As seen in Fig. 5, the magnetic moment approaches to  $\frac{ne}{2m}\hbar$  at all temperatures considered. At low temperatures  $T=0.48$  and 1 K, small oscillations of the magnetic moment are observed in the region of weak magnetic field. These oscillations are getting smoother as the temperature increases and disappear at sufficiently high temperatures.

In Fig. 6, one can see the experimental curve (blue line) obtained for the sample GaAs/AlGaAs at lower temperature 85 mK. The measured concentration of the 2DEG

TABLE II: The experimental (asterisks) [9] and theoretical parameters used in the calculations of the FQHE. MF denotes a magnetic field.

Temperature*, $T$ (K)	Mobility in the absence of MF, $\mu_0^*$ ( $\text{m}^2 / \text{V} \cdot \text{s}$ )	Ratio $\tau/\tau_r$	Functional form of $\mu(B) = \tau_r(B)e/m$
0.48	9	1.95	$(0.11 + 0.056B)^{-1}$
1.00	9	2.84	$(0.11 + 0.064B)^{-1}$
1.65	9	3	$(0.11 + 0.084B)^{-1}$
4.15	9	4.5	$(0.11 + 0.185B)^{-1}$

created in this sample is  $n = 3 \times 10^{15} \text{ m}^{-2}$  and the mobility of charge carriers at  $B = 0$  is  $\mu_0 = 100 \text{ m}^2/\text{V}\cdot\text{s}$ . According to this figure the width of the plateau increases up to 10 Tesla and then suddenly decreases. It starts to increase again from 19 Tesla to 30 Tesla. It is obvious that above 10 Tesla the properties of the system drastically change. In our model this behavior is explained by the abrupt change of the functional form of the mean collision time. Initially being

$$\frac{e}{m}\tau = \frac{80}{1.3 + B}$$

below 19 Tesla (red line), it changes to

$$\frac{e}{m}\tau = \frac{4}{B - 18}$$

above 19 Tesla (black line). The parameter  $\Gamma$  is again set to be  $100/\mu_0$ . It should be noted that the mobility  $\mu = e\tau_r/m = \mu_0$  at  $T = 85 \text{ mK}$  remains constant in a whole range of magnetic field.

As shown, the non-oscillatory term of the conductivity (resistance) plays a key role at high temperature (the classical Hall effect), whereas an oscillatory part mainly contributes to the resistance at low temperature (the quantum Hall and Shubnikov-De Haas effects), where the mobility of charge carriers is sufficiently large and the values of relaxation time and average collision time are comparable. One should stress that the Shubnikov-De Haas, integer and fractional quantum Hall effects are the results of the transitional processes. Note that for the integer and fractional quantum Hall effects, the values of relaxation time and average collision time should be comparable.

#### D. Shubnikov-De Haas effect

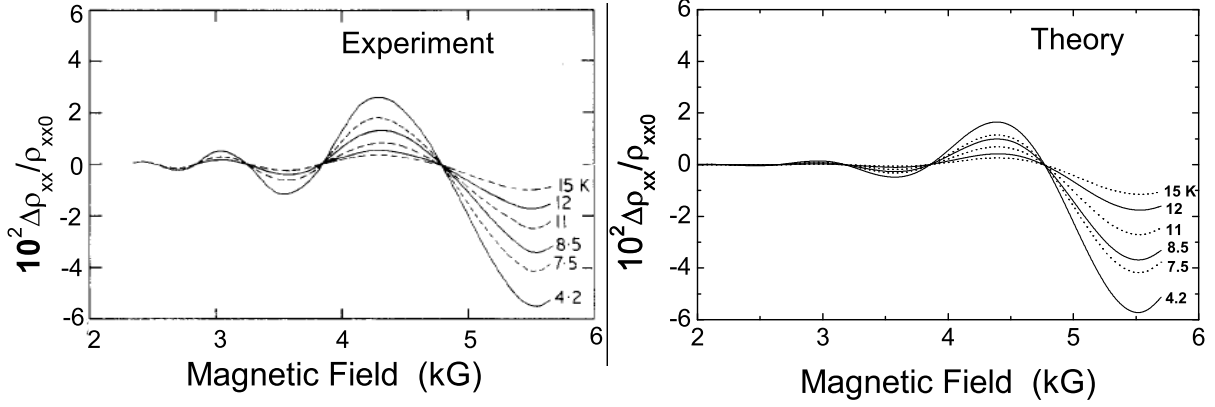


FIG. 7: The experimental [6] and theoretical dependencies of the oscillatory part of the longitudinal magneto-resistance on magnetic field for various temperatures.

Let us consider the experiment performed in Ref. [6] with the  $n$ -InSb sample which has been prepared from the  $n$ -type single crystal of InSb having a charge carrier concentration  $n = 5.9 \cdot 10^{15} \text{ cm}^{-3}$  (see Fig. 7). According to the experiment, the mobility of charge carriers in the absence of magnetic field varies within 5% with increasing temperature from 4.2 to 15 K. However, this value does not show a variation with increasing magnetic field. The points of intersection between the zero axis and the resistance curves are the same at all temperatures. This implies that the period of oscillations does not depend on temperature. Moreover, the equal increase in period of oscillations with the magnetic field is observed at all temperatures in the experiment. So, contrary to the cases of integer and fractional Hall effects, the mobility  $\mu$  or relaxation time  $\tau_r$  of charge carriers in the sample does not change with magnetic field while the mean free time decreases similarly as the magnetic field increases at any temperature. Thus, the ratio of the mean collision time and the relaxation time, which remains constant in the quantum Hall regimes, now decreases with increasing field (see Table III and Fig. 7). No oscillations have been detected in the magnetic field dependence of transverse resistance in the experiment. Though there are oscillations in our approach (Fig. 8), their amplitudes are negligible with respect to the non-oscillatory part of the resistance. In order to detect them, the non-oscillatory part should be subtracted from the measured value as  $\Delta\rho_{xy} = \rho_{xy} - \frac{B}{ne}$ . The calculations of the magnetic moment do not show the oscillations in Fig. 9. The absolute value of magnetic moment decreases with

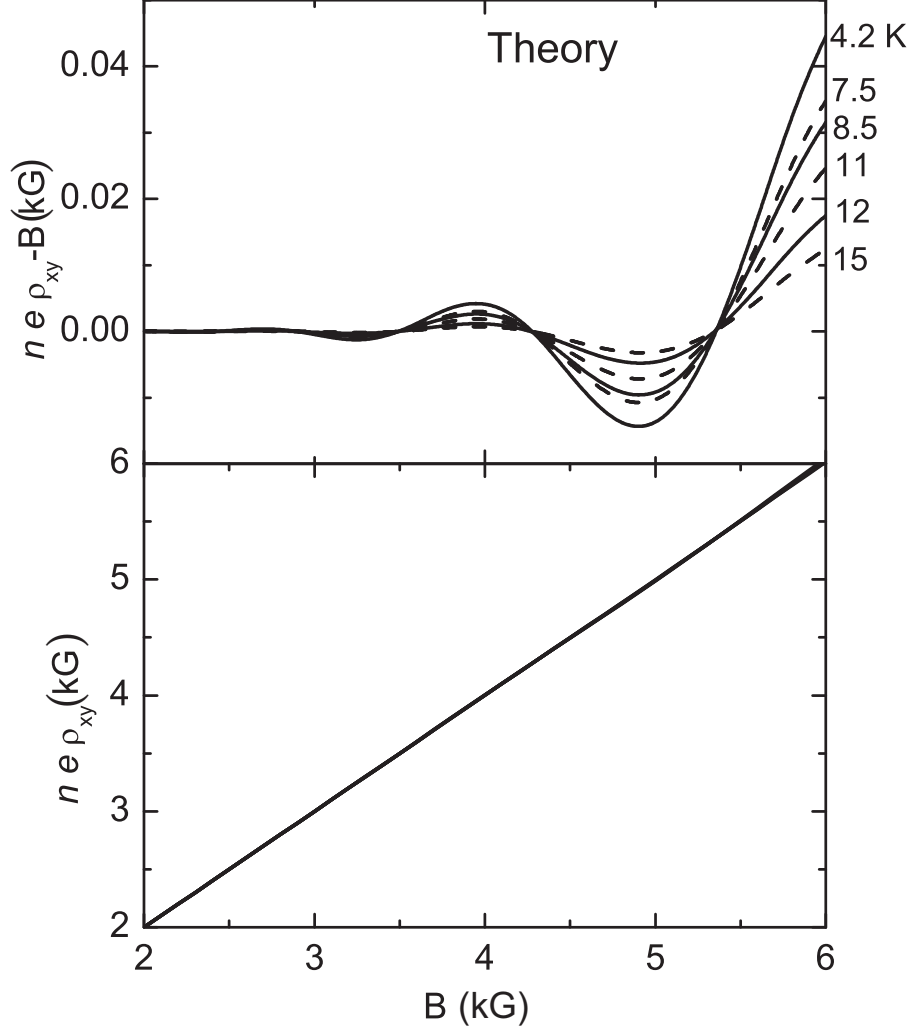


FIG. 8: The dependence of the calculated cross resistance on magnetic field at various temperatures.

TABLE III: The experimental (asterisks) [6] and theoretical parameters used in the calculations of Shubnikov-De Haas effect. MF denotes a magnetic field.

Temperature*, $T$ (K)	4.2	7.5	8.5	11	12	15
Mobility in the absence of MF, $\mu_0^*$ ( $\text{m}^2 / \text{V} \cdot \text{s}$ )	9.5	9.1	8.8	8.4	8.3	8
Functional form of $\tau(B)e/m$	1000/(1.9+12.8 B)					
$\Gamma$	100/ $\mu_0$					

increasing magnetic field.

In Fig. 10, the dependencies of the longitudinal thermal resistance  $k_{xx} = \frac{\chi_{xx}}{\chi_{xx}^2 + \chi_{xy}^2}$  on



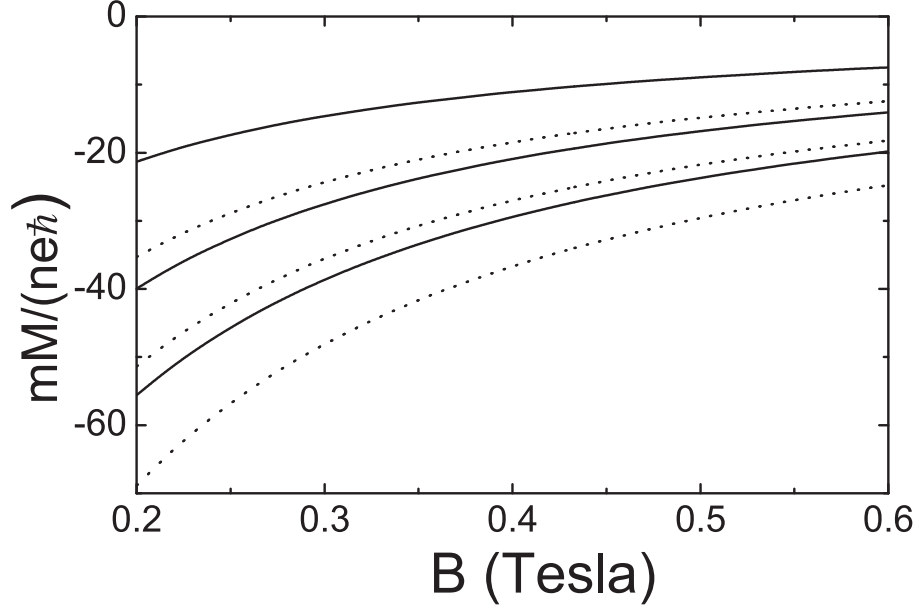


FIG. 9: The calculated magnetic field dependence of the magnetic moment. The curves from top to bottom correspond to the calculations at temperatures  $T=4.2, 7.5, 8.5, 11, 12,$  and  $15$  K.

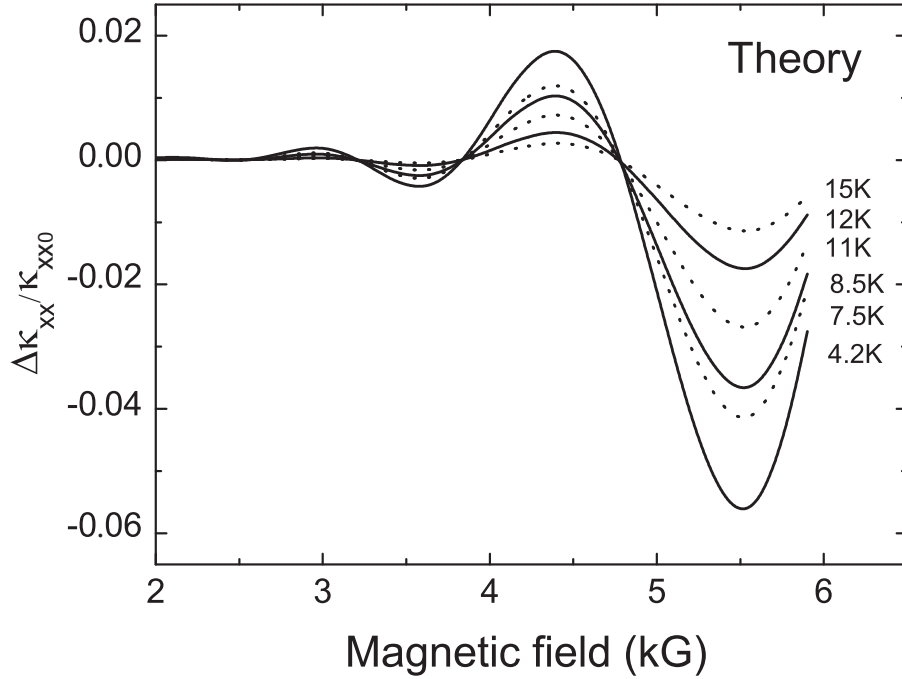


FIG. 10: The calculated dependencies of the oscillatory part of the longitudinal thermal-resistance on magnetic field for various temperatures.

magnetic field are presented at different temperatures. Comparing Figs. 7 and 10, one can

notice the correlations between magneto- and thermal-resistances.

#### IV. SUMMARY

Using the non-Markovian Langevin approach and coupling between the charge carriers and environment, the behavior of the generated flow of charge carriers under the influence of external magnetic field was investigated for the two-dimensional case. The model developed was applied to the case where the collective coordinates are linearly coupled to the heat-bath coordinates. In order to average the influence of environment on the collective system, we applied the spectral function of heat-bath excitations which describes the Drude dissipation with Lorentzian cutoffs. The dynamics of charge carriers was limited by the average collision time as in the kinetic theory of gases. In this way, the two-body effects were taken effectively into consideration. The functional dependencies of the average collision time and coupling strength between the charge carriers and environment on temperature and magnetic field were phenomenologically treated. One can say that we solve the inverse problem by finding suitable coupling strengths and the average collision times for describing the experimental data. As shown, the galvano- and thermo-magnetic effects strongly depend on the ratio between the relaxation time (the inverse friction coefficient) and average collision time.

The explicit expressions were obtained for the macroscopically observable values such as transverse and longitudinal components of conductivity (resistance) and the Hall angle. It was concluded that the non-oscillatory term of conductivity (resistance) plays a key role at high temperature (the classical Hall effect) whereas the oscillatory part of conductivity (resistance) mainly contributes to the resistance at low temperature (quantum Hall and Shubnikov-De Haas effects), where the mobility of charge carriers is sufficiently large and the values of relaxation time and average collision time are comparable. Thus, the Shubnikov-De Haas, integer and fractional quantum Hall effects are the results of the transitional processes.

The Shubnikov-De Haas effect has been observed both in the two-dimensional and three-dimensional samples, whereas the integer and fractional quantum Hall effects have been detected only in the two-dimensional samples so far. However, our model also predicts their existence in the three-dimensional samples. The model was applied to the thermomagnetic processes as well. The oscillations of the thermal coefficients were predicted in the quantum Hall and Shubnikov-De Haas regimes. The experimental observation of such oscillations

would be a good criteria for the justification of the present model.

The model developed can be extended further by taking the spin of electrons and non-stationary external fields into consideration.

### Acknowledgments

This work was partially supported by the Russian Foundation for Basic Research (Moscow) and DFG (Bonn). The IN2P3(France)-JINR(Dubna) Cooperation Programme is gratefully acknowledged.

### Appendix A: The case of two charge carriers

In the case of two kinds of charge carriers, for example electrons and holes, in the current two-band model, we should solve the equations of motion (8) for each kind of charge carriers. The total conductivity tensor consists of the sum of conductivity tensors of transmission electrons and holes

$$\sigma(\tau) = e^2 \begin{pmatrix} \frac{C_3^e(\tau)n_e}{m_x^e} + \frac{C_3^h(\tau)n_h}{m_x^h} & -\frac{D_3^h(\tau)n_h}{m_y^h} + \frac{D_3^e(\tau)n_e}{m_y^e} \\ \frac{\tilde{D}_3^h(\tau)n_h}{m_x^h} - \frac{\tilde{D}_3^e(\tau)n_e}{m_x^e} & \frac{\tilde{C}_3^e(\tau)n_e}{m_y^e} + \frac{\tilde{C}_3^h(\tau)n_h}{m_y^h} \end{pmatrix}, \quad (\text{A1})$$

where  $n_e$  ( $m_{x,y}^e$ ) and  $n_h$  ( $m_{x,y}^h$ ) are the concentrations (the components of the effective mass tensor) of electrons and holes, respectively. Performing the inverse operation on  $\sigma(\tau)$ , we find the magneto-resistance tensor:

$$\rho(\tau) = \frac{1}{\Delta(\tau)} \times \begin{pmatrix} m_x^e m_x^h [m_y^e n_h \tilde{C}_3^h(\tau) + m_y^h n_e \tilde{C}_3^e(\tau)] & m_x^e m_x^h [m_y^e n_h D_3^h(\tau) - m_y^h n_e D_3^e(\tau)] \\ -m_y^e m_y^h [m_x^e n_h \tilde{D}_3^h(\tau) - m_x^h n_e \tilde{D}_3^e(\tau)] & m_y^e m_y^h [m_x^e n_h C_3^h(\tau) + m_x^h n_e C_3^e(\tau)] \end{pmatrix}, \quad (\text{A2})$$

where

$$\Delta(\tau) = e^2 ([m_x^e n_h C_3^h(\tau) + m_x^h n_e C_3^e(\tau)] [m_y^e n_h \tilde{C}_3^h(\tau) + m_y^h n_e \tilde{C}_3^e(\tau)] + [m_y^e n_h D_3^h(\tau) - m_y^h n_e D_3^e(\tau)] [m_x^e n_h \tilde{D}_3^h(\tau) - m_x^h n_e \tilde{D}_3^e(\tau)]).$$

The Hall resistance takes the following form

$$\begin{aligned} \rho_H(\tau) &= \frac{m_x^e m_x^h [m_y^h n_e D_3^e(\tau) - m_y^e n_h D_3^h(\tau)]}{\Delta(\tau)} \\ &= \frac{m_y^e m_y^h [m_x^h n_e \tilde{D}_3^e(\tau) - m_x^e n_h \tilde{D}_3^h(\tau)]}{\Delta(\tau)}. \end{aligned} \quad (\text{A3})$$

## Appendix B: Variances

The equations for the second moments (variances),

$$\Sigma_{q_i q_j}(t) = \frac{1}{2} \langle q_i(t) q_j(t) + q_j(t) q_i(t) \rangle - \langle q_i(t) \rangle \langle q_j(t) \rangle,$$

where  $q_i = x, y, \pi_x$ , or  $\pi_y$  ( $i=1-4$ ), are

$$\begin{aligned} \dot{\Sigma}_{xx}(t) &= \frac{2\Sigma_{x\pi_x}(t)}{m_x}, & \dot{\Sigma}_{yy}(t) &= \frac{2\Sigma_{y\pi_y}(t)}{m_y}, \\ \dot{\Sigma}_{xy}(t) &= \frac{\Sigma_{x\pi_y}(t)}{m_y} + \frac{\Sigma_{y\pi_x}(t)}{m_x}, \\ \dot{\Sigma}_{x\pi_y}(t) &= -\lambda_{\pi_y}(t)\Sigma_{x\pi_y}(t) - \tilde{\omega}_{cx}(t)\Sigma_{x\pi_x}(t) + \frac{\Sigma_{\pi_x\pi_y}(t)}{m_x} + 2D_{x\pi_y}(t), \\ \dot{\Sigma}_{x\pi_x}(t) &= -\lambda_{\pi_x}(t)\Sigma_{x\pi_x}(t) + \tilde{\omega}_{cy}(t)\Sigma_{x\pi_y}(t) + \frac{\Sigma_{\pi_x\pi_x}(t)}{m_x} + 2D_{x\pi_x}(t), \\ \dot{\Sigma}_{y\pi_x}(t) &= -\lambda_{\pi_x}(t)\Sigma_{y\pi_x}(t) + \tilde{\omega}_{cy}(t)\Sigma_{y\pi_y}(t) + \frac{\Sigma_{\pi_x\pi_y}(t)}{m_y} + 2D_{y\pi_x}(t), \\ \dot{\Sigma}_{y\pi_y}(t) &= -\lambda_{\pi_y}(t)\Sigma_{y\pi_y}(t) - \tilde{\omega}_{cx}(t)\Sigma_{y\pi_x}(t) + \frac{\Sigma_{\pi_y\pi_y}(t)}{m_y} + 2D_{y\pi_y}(t), \\ \dot{\Sigma}_{\pi_y\pi_y}(t) &= -2\lambda_{\pi_y}(t)\Sigma_{\pi_y\pi_y}(t) - 2\tilde{\omega}_{cx}(t)\Sigma_{\pi_x\pi_y}(t) + 2D_{\pi_y\pi_y}(t), \\ \dot{\Sigma}_{\pi_x\pi_x}(t) &= -2\lambda_{\pi_x}(t)\Sigma_{\pi_x\pi_x}(t) + 2\tilde{\omega}_{cy}(t)\Sigma_{\pi_x\pi_y}(t) + 2D_{\pi_x\pi_x}(t), \\ \dot{\Sigma}_{\pi_x\pi_y}(t) &= -(\lambda_{\pi_x}(t) + \lambda_{\pi_y}(t))\Sigma_{\pi_x\pi_y}(t) + \tilde{\omega}_{cy}(t)\Sigma_{\pi_y\pi_y}(t) - \tilde{\omega}_{cx}(t)\Sigma_{\pi_x\pi_x}(t) + 2D_{\pi_x\pi_y}(t) \end{aligned} \quad (\text{B1})$$

So, we obtain the Markovian-type (local in time) equations for the first and second moments, but with the transport coefficients depending explicitly on time. The time-dependent diffu-

sion coefficients  $D_{q_i q_j}(t)$  are determined as

$$\begin{aligned}
D_{xx}(t) &= D_{yy}(t) = D_{xy}(t) = 0, \\
D_{\pi_x \pi_x}(t) &= \lambda_{\pi_x}(t) J_{\pi_x \pi_x}(t) - \tilde{\omega}_{cy}(t) J_{\pi_x \pi_y}(t) + \frac{1}{2} \dot{J}_{\pi_x \pi_x}(t), \\
D_{\pi_y \pi_y}(t) &= \lambda_{\pi_y}(t) J_{\pi_y \pi_y}(t) + \tilde{\omega}_{cx}(t) J_{\pi_x \pi_y}(t) + \frac{1}{2} \dot{J}_{\pi_y \pi_y}(t), \\
D_{\pi_x \pi_y}(t) &= -\frac{1}{2} \left[ -(\lambda_{\pi_x}(t) + \lambda_{\pi_y}(t)) J_{\pi_x \pi_y}(t) + \tilde{\omega}_{cy}(t) J_{\pi_y \pi_y}(t) - \tilde{\omega}_{cx}(t) J_{\pi_x \pi_x}(t) - \dot{J}_{\pi_x \pi_y}(t) \right], \\
D_{x\pi_y}(t) &= -\frac{1}{2} \left[ -\lambda_{\pi_y}(t) J_{x\pi_y}(t) - \tilde{\omega}_{cx}(t) J_{x\pi_x}(t) + \frac{J_{\pi_x \pi_y}(t)}{m_x} - \dot{J}_{x\pi_y}(t) \right], \\
D_{y\pi_x}(t) &= -\frac{1}{2} \left[ -\lambda_{\pi_x}(t) J_{y\pi_x}(t) + \tilde{\omega}_{cy}(t) J_{y\pi_y}(t) + \frac{J_{\pi_x \pi_y}(t)}{m_y} - \dot{J}_{y\pi_x}(t) \right], \\
D_{x\pi_x}(t) &= -\frac{1}{2} \left[ -\lambda_{\pi_x}(t) J_{x\pi_x}(t) + \tilde{\omega}_{cy}(t) J_{x\pi_y}(t) + \frac{J_{\pi_x \pi_x}(t)}{m_x} - \dot{J}_{x\pi_x}(t) \right], \\
D_{y\pi_y}(t) &= -\frac{1}{2} \left[ -\lambda_{\pi_y}(t) J_{y\pi_y}(t) - \tilde{\omega}_{cx}(t) J_{y\pi_x}(t) + \frac{J_{\pi_y \pi_y}(t)}{m_y} - \dot{J}_{y\pi_y}(t) \right]. \tag{B2}
\end{aligned}$$

Here,  $\dot{J}_{q_i q_j}(t) = dJ_{q_i q_j}(t)/dt$  and

$$\begin{aligned}
J_{xx}(t) &= \ll I_x(t) I_x(t) + I'_x(t) I'_x(t) \gg, \quad J_{yy}(t) = J_{xx}(t)|_{x \rightarrow y}, \\
J_{xy}(t) &= \ll I_x(t) I_y(t) + I'_x(t) I'_y(t) \gg, \quad J_{\pi_x \pi_y}(t) = J_{xy}(t)|_{x \rightarrow \pi_x, y \rightarrow \pi_y}, \\
J_{x\pi_x}(t) &= \ll I_x(t) I_{\pi_x}(t) + I'_x(t) I'_{\pi_x}(t) \gg, \quad J_{y\pi_x}(t) = J_{x\pi_x}(t)|_{x \rightarrow y}, \\
J_{x\pi_y}(t) &= \ll I_x(t) I_{\pi_y}(t) + I'_x(t) I'_{\pi_y}(t) \gg, \quad J_{y\pi_y}(t) = J_{x\pi_y}(t)|_{x \rightarrow y}, \\
J_{\pi_x \pi_x}(t) &= \ll I_{\pi_x}(t) I_{\pi_x}(t) + I'_{\pi_x}(t) I'_{\pi_x}(t) \gg, \quad J_{\pi_y \pi_y}(t) = J_{\pi_x \pi_x}(t)|_{\pi_x \rightarrow \pi_y}. \tag{B3}
\end{aligned}$$

The explicit expressions for  $J_{q_i q_j}(t)$  are

$$\begin{aligned}
J_{xx}(t) &= \frac{m\hbar\gamma^2}{\pi} \int_0^\infty d\omega \int_0^t dt' \int_0^t dt'' \frac{\omega \coth \left[ \frac{\hbar\omega}{2T} \right]}{\omega^2 + \gamma^2} \\
&\quad \times [\lambda_x A_1(t') A_1(t'') + \lambda_y A_2(t') A_2(t'')] \cos(\omega[t'' - t']), \\
J_{xy}(t) &= \frac{m\hbar\gamma^2}{\pi} \int_0^\infty d\omega \int_0^t dt' \int_0^t dt'' \frac{\omega \coth \left[ \frac{\hbar\omega}{2T} \right]}{\omega^2 + \gamma^2} \\
&\quad \times [\lambda_x A_1(t') B_2(t'') + \lambda_y A_2(t') B_1(t'')] \cos(\omega[t'' - t']), \\
J_{\pi_x \pi_x}(t) &= \frac{m\hbar\gamma^2}{\pi} \int_0^\infty d\omega \int_0^t dt' \int_0^t dt'' \frac{\omega \coth \left[ \frac{\hbar\omega}{2T} \right]}{\omega^2 + \gamma^2} \\
&\quad \times [\lambda_x C_1(t') C_1(t'') + \lambda_y C_2(t') C_2(t'')] \cos(\omega[t'' - t']),
\end{aligned}$$

$$\begin{aligned}
J_{\pi_x \pi_y}(t) &= \frac{m\hbar\gamma^2}{\pi} \int_0^\infty d\omega \int_0^t dt' \int_0^t dt'' \frac{\omega \coth \left[ \frac{\hbar\omega}{2T} \right]}{\omega^2 + \gamma^2} \\
&\quad \times [\lambda_x C_1(t') D_2(t'') + \lambda_y C_2(t') D_1(t'')] \cos(\omega[t'' - t']), \\
J_{x\pi_x}(t) &= \frac{m\hbar\gamma^2}{\pi} \int_0^\infty d\omega \int_0^t dt' \int_0^t dt'' \frac{\omega \coth \left[ \frac{\hbar\omega}{2T} \right]}{\omega^2 + \gamma^2} \\
&\quad \times [\lambda_x A_1(t') C_1(t'') + \lambda_y A_2(t') C_2(t'')] \cos(\omega[t'' - t']), \\
J_{x\pi_y}(t) &= \frac{m\hbar\gamma^2}{\pi} \int_0^\infty d\omega \int_0^t dt' \int_0^t dt'' \frac{\omega \coth \left[ \frac{\hbar\omega}{2T} \right]}{\omega^2 + \gamma^2} \\
&\quad \times [\lambda_x A_1(t') D_2(t'') + \lambda_y A_2(t') D_1(t'')] \cos(\omega[t'' - t']).
\end{aligned}$$

In our treatment  $D_{xx} = D_{yy} = D_{xy} = 0$ , because there are no random forces for  $x$  and  $y$  coordinates in Eqs. (8). At  $\omega_{cx} = \omega_{cy} = 0$ , we have  $D_{y\pi_x}(t) = D_{x\pi_y}(t) = D_{\pi_x \pi_y}(t) = 0$ .

- 
- [1] S.V. Vonsowsky, *Magnetism* (Nauka Publishers, Moscow, 1971) p.313.
  - [2] Ch. Kittel, *Quantum Theory of Solids* (John Wiley & Sons, Inc., USA, 1987).
  - [3] Ch. Kittel, *Introduction to Solid State Physics* Ch.12, 7-th Ed. (Wiley, Singapore, 1996).
  - [4] E.S. Borovik, Doklady Acad. Nauk S.S.S.R. **70**, 601 (1950).
  - [5] K.F. Komatsubara, Phys. Rev. Lett. **16**, 1044 (1966).
  - [6] G. Bauer and H. Kahlert, J. Phys. C: Solid State Phys. **6**, 1253 (1973).
  - [7] K. von Klitzing, G. Dorda, and M. Pepper, Phys. Rev. Lett. **45**, 494 (1980).
  - [8] G.Ebert, K. von Klitzing, C.Probst, and K.Ploog, Sol. State Comm. **44**, 95 (1982).
  - [9] D.C. Tsui, H.L. Störmer, and A.C. Gossard, Phys. Rev. Lett. **48**, 1559 (1982).
  - [10] R. Willet, J.P. Eisenstein, H.L. Störmer, D.C. Tsui, A.C. Gossard, and J.H. English, Phys. Rev. Lett. **59**, 1776 (1987).
  - [11] R.E. Prange and S.M. Girvin, *The Quantum Hall Effect* (Springer-Verlag, New York, 1990).
  - [12] R.B. Laughlin, Phys. Rev. Lett. **50**, 1395 (1983).
  - [13] F.D.M. Haldane, Phys. Rev. Lett. **51**, 605 (1983).
  - [14] B.I. Halperin, Phys. Rev. Lett. **52**, 1583; 2390(E) (1983).
  - [15] J.K. Jain, Phys. Rev. Lett. **63**, 199 (1989).
  - [16] A.A. Belavin, A.M. Polyakov, and A.B. Zamolodchikov, Nucl. Phys. B **241**, 333 (1984).
  - [17] J. Fröhlich and A. Zee, Nucl. Phys. B **364**, 517 (1991).

- [18] V. Kač and A. Radul, *Comm. Math. Phys.* **157**, 429 (1993).
- [19] D. Karabali, *Nucl. Phys. B* **419**, 437 (1994); *Nucl. Phys. B* **428**, 531 (1994).
- [20] N.G. van Kampen, *Stochastic Processes in Physics and Chemistry* (North-Holland, Amsterdam, 1981).
- [21] C.W. Gardiner, *Quantum Noise* (Springer, Berlin, 1991).
- [22] U. Weiss, *Quantum Dissipative Systems* (Wold Scientific, Singapore, 1999).
- [23] D. Zubarev, V. Morozov, and G. Röpke, *Statistical mechanics of nonequilibrium processes*, Vol. 2 (Academie Verlag, Berlin, 1997) p. 52.
- [24] H.J. Carmichael, *An open system approach to quantum optics* (Springer, Berlin, 1993).
- [25] Yu.L. Klimontovich, *Statistical theory of open systems* (Kluwer Academic Publishers, Dordrecht, 1995).
- [26] A.O. Caldeira and A.J. Leggett, *Phys. Rev. Lett.* **46**, 211 (1981); *Phys. Rev. Lett.* **48**, 1571 (1982); *Ann. Phys. (N.Y.)* **149**, 374 (1983).
- [27] V. V. Dodonov and V. I. Man'ko, *Density Matrices and Wigner Functions of Quasiclassical Quantum Systems*, Proc. Lebedev Phys. Inst. of Sciences, Vol. **167**, ed. A. A. Komar (Nova Science, Commack, N. Y., 1987).
- [28] K. Lindenberg and B. J. West, *The Nonequilibrium Statistical Mechanics of Open and Closed* (VCH Publishers, Inc., New York, 1990); K. Lindenberg and B. J. West, *Phys. Rev. A* **30**, 568 (1984).
- [29] A. Isar, A. Sandulescu, H. Scutaru, E. Stefanescu, and W. Scheid, *Int. J. Mod. Phys. E* **3**, 635 (1994).
- [30] G.W. Ford, J.T. Lewis, and R.F. O'Connell, *Phys. Rev. A* **36**, 1466 (1987); *A* **37**, 4419 (1988).
- [31] G.Y. Hu and R.F. O'Connell, *Physica A* **151**, 33 (1988); *Phys. Rev. B* **36**, 5798 (1987).
- [32] X.L. Li, G.W. Ford, and R.F. O'Connell, *Phys. Rev. A* **41**, 5287 (1990); *ibid* **42**, 4519 (1990); *Physica A* **193**, 575 (1993).
- [33] X.L. Li, G.W. Ford, and R.F. O'Connell, *Phys. Rev. E* **53**, 3359 (1996).
- [34] S. Dattagupta and J. Singh, *Phys. Rev. Lett.* **79**, 961 (1997).
- [35] Th.M. Nieuwenhuizen and A.E. Allahverdyan, *Phys. Rev. E* **66**, 036102 (2002).
- [36] Z. Kanokov, Yu.V. Palchikov, G.G. Adamian, N.V. Antonenko, and W. Scheid, *Phys. Rev. E* **71**, 016121 (2005); Sh.A. Kalandarov, Z. Kanokov, G.G. Adamian, and N.V. Antonenko, *Phys. Rev. E* **75**, 0311115 (2007).

- [37] G.G. Adamian, N.V. Antonenko, Z. Kanokov, and V.V. Sargsyan, *Theor. Math. Phys.* **145**, 1443 (2005).
- [38] V.V. Sargsyan, Z. Kanokov, G.G. Adamian, and N.V. Antonenko, *Phys. Rev. C* **77**, 024607 (2008).
- [39] V.V. Sargsyan, Z. Kanokov, G.G. Adamian, and N.V. Antonenko, *Phys. Part. Nuclei* **41**, 175 (2010).
- [40] R.A. Kuzyakin, V.V. Sargsyan, G.G. Adamian, and N.V. Antonenko, *Phys. Rev. A* **83**, 062117 (2011); **84**, 032117 (2011).
- [41] K. Wen, F. Sakata, Z.-X. Li, X.-Z. Wu, Y.-X. Zhang, and S.-G. Zhou, *Phys. Rev. Lett.* **111**, 012501 (2013).
- [42] V.V. Sargsyan, D. Lacroix, G.G. Adamian, and N.V. Antonenko, *Phys. Rev. A* **90**, 022123 (2014).
- [43] D. Lacroix, V.V. Sargsyan, G.G. Adamian, and N.V. Antonenko, *Eur. Phys. J. B* **88**, 89 (2015).
- [44] V.V. Sargsyan, D. Lacroix, G.G. Adamian, and N.V. Antonenko, *Phys. Rev. A* **95**, 032119 (2017).
- [45] V.V. Sargsyan, D. Lacroix, G.G. Adamian, and N.V. Antonenko, *Phys. Rev. A* **96**, 012114 (2017).
- [46] A.A. Hovhannisyan, V.V. Sargsyan, G.G. Adamian, N.V. Antonenko, and D. Lacroix, *Phys. Rev. E* **97**, 032134 (2018).
- [47] V.V. Sargsyan, A.A. Hovhannisyan, G.G. Adamian, N.V. Antonenko, and D. Lacroix, *Physica A* **505**, 666 (2018).